



UNIVERSITY OF LEEDS

This is a repository copy of *n-Si/SiGe quantum cascade structures for THz emission*.

White Rose Research Online URL for this paper:

<http://eprints.whiterose.ac.uk/1672/>

Article:

Ikonic, Z., Lazic, I., Milanovic, V. et al. (3 more authors) (2006) n-Si/SiGe quantum cascade structures for THz emission. *Journal of Luminescence*, 121 (2). pp. 311-314. ISSN 0022-2313

<https://doi.org/10.1016/j.jlumin.2006.08.049>

Reuse

See Attached

Takedown

If you consider content in White Rose Research Online to be in breach of UK law, please notify us by emailing eprints@whiterose.ac.uk including the URL of the record and the reason for the withdrawal request.



eprints@whiterose.ac.uk
<https://eprints.whiterose.ac.uk/>



White Rose
university consortium
Universities of Leeds, Sheffield & York

White Rose Consortium ePrints Repository

<http://eprints.whiterose.ac.uk/>

This is an author produced version of a paper published in **Journal of Luminescence**.

White Rose Repository URL for this paper:

<http://eprints.whiterose.ac.uk/1672/>

Published paper

Ikonic, Z., Lazic, I., Milanovic, V., Kelsall, R.W., Indjin, D. and Harrison, P. (2006) *n-Si/SiGe quantum cascade structures for THz emission*. Journal of Luminescence, 121 (2). pp. 311-314.

Published in Journal of Luminescence, **121**, 311-314 (2006)

n-Si/SiGe quantum cascade structures for THz emission

Z. Ikonic¹⁾, I. Lazic^{2,3)}, V. Milanovic²⁾, R. W. Kelsall¹⁾, D. Indjin¹⁾, and P. Harrison¹⁾

¹⁾School of Electronic and Electrical Engineering, University of Leeds, Leeds, LS2 9JT, United Kingdom

²⁾School of Electrical Engineering, University of Belgrade, Belgrade, Yugoslavia

³⁾Department of Materials Science, Delft University of Technology, 2628 AL Delft, Netherlands

Abstract

In this work we report on modelling the electron transport in n-Si/SiGe structures. The electronic structure is calculated within the effective-mass complex-energy framework, separately for perpendicular (X_z) and in-plane (X_{xy}) valleys, the degeneracy of which is lifted by strain, and additionally by size quantization. The transport is described via scattering between quantized states, using the rate equations approach and tight-binding expansion, taking the coupling with two nearest-neighbour periods. The acoustic phonon, optical phonon, alloy and interface roughness scattering are taken in the model. The calculated U/I dependence and gain profiles are presented for a couple of QC structures.

1. Introduction

Following the successful realization of GaAs/AlGaAs based THz quantum cascade lasers, Si/SiGe quantum cascade structures are attracting considerable attention as a very promising technology for the same purpose. This would offer compatibility and even monolithic integration with the standard CMOS technology. Within the Si/SiGe system, the p-doped structures have been explored in more detail, because of larger discontinuity of the valence band at heterointerfaces. For THz emission, however, even modest discontinuities would suffice, which makes n-doped structures just as interesting, and here we report on modeling the electron transport and light emission in n-Si/SiGe cascades. We have previously made extensive modelling of hole transport [1], demonstrated the growth of p-Si/SiGe strain-symmetrized cascades with up to 1200 layers, and observed THz electroluminescence from them [2]. Mid-infrared luminescence has been observed by another group [3]. In this paper we consider electron transport in n-doped Si/SiGe cascades. This is quite different from transport in n-doped GaAs/AlGaAs cascades, both because one of the major scattering processes – polar LO-phonon scattering – does not exist in Si/SiGe, and because of the presence of two types of quantized electronic states.

2. Theory and computational details

$\text{Si}_{1-x}\text{Ge}_x$ alloys with $x < 0.85$ are similar to the silicon, in that the conduction band minima appear near the X point of the Brillouin zone. Accordingly, the low-lying conduction band quantized states in a Si/SiGe multilayer structure originate from the six X valleys, and depend on the potential experienced by electrons in these valleys. The X

valleys are anisotropic, having different longitudinal and transverse effective mass. To find the electronic subband structure we employ the effective mass envelope function Schrodinger equation description. For structures grown on the conventional, [001] oriented substrate, two X valleys with axis parallel to the growth direction (denoted as X_z) give rise to quantized subbands different from those of four X valleys whose axes are perpendicular to the growth direction (denoted as X_{xy}). This is because the quantization effective masses are different in the two cases, amounting to $m_l = 0.916m_e$ and $m_t = 0.19m_e$ in both materials, where m_e is the free electron mass. Furthermore, the different lattice constants of Si and Ge imply that layers in Si/SiGe cascade have to be uniaxially strained, the amount of strain being set by the choice of the substrate composition (Ge molar fraction x_s), in turn chosen so to achieve strain balance. The in-plane lattice constant of epilayer material equals that of the substrate, while the perpendicular lattice constant changes. The strain lifts the degeneracy between the six X valleys, and hence also influences the subband energies. The potential energy (position of the X valley bottom) in a strained $\text{Si}_{1-x}\text{Ge}_x$ alloy layer, measured from the valence band top of the substrate, is calculated according to [4]

$$E_{cond}^X = -\frac{\Delta_{so}(x_s)}{3} + \Delta E_{v,av}(x, x_s) - \Delta E_{v,av,hyd}(x, x_s) + \frac{\Delta_{so}(x)}{3} + E_g(x) + \Delta E_{hyd}^H(x, x_s) + \Delta E_{uni}^X(x, x_s) \quad (1)$$

where X stands for either X_z or X_{xy} , Δ_{so} is the composition dependent spin-orbit splitting, $\Delta E_{v,av} = (x - x_s) \cdot (0.74 - 0.06 \cdot x_s) [eV]$ is the average valence band offset between relaxed substrate and this alloy, $E_g(x) = 1.17 - 0.34x + 0.206x^2$ is the (experimental) band gap of the alloy, $\Delta E_{v,av,hyd} = a_V(2\varepsilon_{xx} + \varepsilon_{zz})$ is hydrostatic strain component induced change of valence band offset, $\Delta E_{hyd}^H = (\Xi_d + \Xi_u/3)(2\varepsilon_{xx} + \varepsilon_{zz})$ the hydrostatic strain

component induced shift of X valley edge, while $\Delta E_{uni}^{X_z} = 2\Xi_u(\varepsilon_{zz} - \varepsilon_{xx})/3$ and $\Delta E_{uni}^{X_{xy}} = -\Xi_u(\varepsilon_{zz} - \varepsilon_{xx})/3$ are the uniaxial strain component induced shifts of X valley edge (different for the two types of X valleys). The strain components in a layer are given by $\varepsilon_{xx} = \varepsilon_{yy} = a/a_0 - 1$ and $\varepsilon_{zz} = -(2C_{12}/C_{11})\varepsilon_{xx}$, where a_0 and a are lattice constants of unstrained layer and substrate respectively. The lattice constant of an unstrained layer with Ge mole fraction x is given by $a(x) = a_{Ge} \cdot x + a_{Si} \cdot (1-x) - b_{bow} \cdot x \cdot (1-x)$.

The material constants used in this calculation are $a_V = -4.54(-3.1)$, for the germanium and linear interpolation for the $\text{Si}_{1-x}\text{Ge}_x$ alloys, $\Xi_u = 8.6(9.4)$ and $\Xi_d = -6.0(-4.92)$, $C_{11} = 1.675(1.315)$, $C_{12} = 0.650(0.494)$, $a = 0.543(0.565)$ nm for Si (Ge). Linear interpolation is used for the $\text{Si}_{1-x}\text{Ge}_x$ alloy parameters, except for the lattice constant where bowing was taken into account, with $b_{bow} = 0.00188$ 1/nm.

For practically realizable, strain balanced structures, with Si and SiGe layers grown on a substrate with composition in between, the Si layers are quantum wells for both types of electrons (valleys), with X_z valley shifted below and X_{xy} valley above their position in unstrained Si, and the opposite holds for SiGe alloy layers, implying much shallower wells for X_{xy} than for X_z electrons. Combined with the fact that m_l is over 4 times larger than m_t , the few lowest subbands will belong to the X_z valley, and are much more strongly bound than X_{xy} valley subbands.

In biased quantum cascade structures the subbands are not strictly discrete (instead, one has more or less sharp resonances in the continuum), but in most cases, e.g. in conventional III-V based cascades, these are sharp enough that one can solve the Schrodinger equation for discrete states, using box boundary conditions. The shallow

wells present for X_{xy} electrons in Si/SiGe would make such an approach inappropriate. Therefore, we have used the complex energy method [5], which allows subband energies to take complex values and then delivers better-behaved and normalizable resonant state wave functions, which can be more reliably used in scattering rate calculations. The imaginary component of energy here corresponds to the tunneling rate, and in actual structures was usually small enough to be neglected, so only the real part of energy was further used. Among all the states found in a multiple period structure, some are assigned to belong to the reference (“central“) period, based on their localization properties, and then are replicated (shifted in space and energy) to obtain states assigned to the neighbouring periods.

Electrons in the structure change their quantum states by scattering with phonons, on interface roughness, alloy disorder, ionized impurities, carrier-carrier scattering. In this paper we consider the first three mechanisms, and take the small enough doping that the last two can be neglected. Furthermore, we take that photon emission / absorption processes do not contribute significantly to electron transport (cascade operation below lasing threshold). With two equivalent X_z and four equivalent X_{xy} valleys, there are as many sets of degenerate subbands. Some scattering processes cause the electrons to change the valley they belong to (and perhaps also the subband index), and other only act within different subbands of the same valley.

If initial and final states belong to different X valleys, the (intervalley) scattering is caused by large wave vector phonons. Processes in which electron scatters between two X valleys oriented at 90° , e.g. X_{z+} and X_{y+} , are f - processes, and those between two valleys oriented at 180° , e.g. X_{z+} and X_{z-} , are g - processes. It should be noted, therefore,

that two subbands of X_z valley can be coupled by g-processes (e.g. if the initial state belongs to X_{z+} , and the final to X_{z-}). Some of these processes are "allowed" and others are "forbidden". On the other hand, the small-wave vector acoustic phonons only cause transitions between states belonging to the same valley, e.g. both to X_{z+} , and the same is assumed for interface roughness and alloy disorder scattering. The phonon scattering rates are calculated according to [6], and the last two scattering rates according to [7]. The energy-dependent scattering rates are then averaged over the in-plane electron distribution, allowing the electron temperature to differ from the lattice temperature. In numerical calculations we use the parameter values for Si as a good approximation, because this is the well material where most of the wave functions are localized. The phonon scattering parameters were taken from [8], and for the interface roughness scattering we used the values $\Delta=0.4$ nm and $\Lambda=16$ nm.

Denoting with n_i electron concentration in the quantum state i of the "central" period, and explicitly accounting for N such states, we assume the periodicity of electron distribution over periods, i.e. $\dots = n_{i-N} = n_i = n_{i+N} = \dots$ for every $i = 1, 2, \dots, N$, where n_{i-N} and n_{i+N} are densities on state i in the periods nearest to the "central", n_{i-2N} and n_{i+2N} in the second nearest neighbours and, consistent with it, we assume electrical neutrality, $\sum_{i=1}^N n_i = N_D$, where N_D is the donors doping per period. Using the shift-invariance of scattering rates, the rate equations read

$$\begin{aligned} \frac{dn_i}{dt} = & -n_i \sum_{j=1}^N (\omega_{i \rightarrow j} + \omega_{i \rightarrow j+N} + \omega_{i+N \rightarrow j} + \omega_{i \rightarrow j+2N} + \omega_{i+2N \rightarrow j}) + \\ & \sum_{j=1}^N (\omega_{j \rightarrow i} + \omega_{j \rightarrow i+N} + \omega_{j+N \rightarrow i} + \omega_{j \rightarrow i+2N} + \omega_{j+2N \rightarrow i}) \cdot n_j \end{aligned} \quad (2)$$

In the steady state one of the equations is replaced by the electrical neutrality condition. One could add the thermal balance rate equations to find electron distribution of each subband. In the present calculation, however, we did not use such more elaborate model, and electron temperatures were fixed to values larger than the lattice temperature, chosen to lie within the range found in previous calculations in p-Si/SiGe cascades [1].

3. Results and discussion

Numerical calculations were performed for two simple cascade structures: (a) Si(6 nm)/Si_{0.65}Ge_{0.35}(1 nm), and (b) Si(8 nm)/Si_{0.6}Ge_{0.4}(1 nm), both grown on Si_{0.95}Ge_{0.05} substrate. The X_z state spacing in them is in tens of meV range (precise values depending on the bias, but approx. 27 meV and 20 meV between the lowest two states, respectively), and there is just one X_{xy} state localized in the wells, lying between the first and second excited X_z states. The donor doping was assumed to be 10^{11} cm⁻² per period, the carrier temperatures were set to 150 K (a) and 100 K (b), and the lattice temperature to 20 K. The calculated population of states and current are shown in Figs.1 and 2. There clearly exist ranges of bias fields where inversion appears between some two subsequent X_z states (i.e. where the transition matrix element can be significant). To be sustainable and useful, however, the operating point of the cascade should not be in the range where the differential resistance is negative, otherwise one can expect domain formation which would drive the cascade out of such operating point. A closer look at Figs.1 and 2 shows that there are, albeit narrow, bias ranges where the population inversion coexisting with stable operation appears possible.

The calculated fractional gain / absorption profiles for the two cascades biased at suitably chosen fields is shown in Fig.3, with the linewidth (FWHM) of 10 meV was assumed. This amounts to gain coefficients of 18.6 cm^{-1} at photon energy of 27 meV for structure (a), and 4.4 cm^{-1} at 21 meV for structure (b), the former being in practically interesting range. The gain scales linearly with the doping density, but additional scattering mechanisms which were here neglected (carrier-carrier, and ionized impurity scattering) would have to be included in calculation for large values of doping. Certainly, further improvements should be expected from more complex structure of the cascade period.

4. Conclusion

We have considered electron transport in n-Si/SiGe cascade structures, using the rate equations approach and tight-binding expansion, taking the coupling with two nearest-neighbour periods. The acoustic phonon, optical phonon, alloy and interface roughness scattering are taken in the model. The calculated U/I dependence and gain profiles are presented for a couple of QC structures. The existence of technically significant gain, together with positive differential resistance in narrow ranges of bias fields is predicted.

Acknowledgement

The authors are grateful to the Royal Society (UK) for support.

References

- [1] Z. Ikonic, P. Harrison, and R. W. Kelsall, *J. Appl. Phys.*, 96 (2004) 6803.
- [2] R. Bates, et al., *Appl. Phys. Lett.*, 83 (2003) 4092.
- [3] G. Dehlinger, et al., *Science*, 290 (2000) 2277.
- [4] G. Curatola, and G. Iannaccone, *Nanotechnology*, 13 (2002) 267.
- [5] M. Wagner, and H. Mizuta, *Phys. Rev. B*, 48 (1993) 14402.
- [6] F. Monsef, P. Dollfus, S. Galdin, and A. Bournel, *Phys. Rev. B*, 65 (2002) 212304;
Phys. Rev. B, 67 (2003) 059903.
- [7] T. Unuma, M. Yoshita, T. Noda, H. Sakaki, and H. Akiyama, *J. Appl. Phys.*, 93 (2003) 1586.
- [8] P. Dollfus, *J. Appl. Phys.*, 82 (1997) 3911.

Figure captions

Fig.1. The population of four lowest X_z subbands (solid lines) and the X_{xy} subband (dot-dashed line), and the current density (dashed line) calculated for Si/SiGe cascade structure (a) described in the text.

Fig.2. Same as in Fig.1, but for the structure (b).

Fig.3. The fractional (per period) gain / absorption profile calculated for the cascade (a) biased at 43 kV/cm (dashed line), and cascade (b) biased at 56 kV/cm (solid line). The luminescence line FWHM was set to 10 meV.

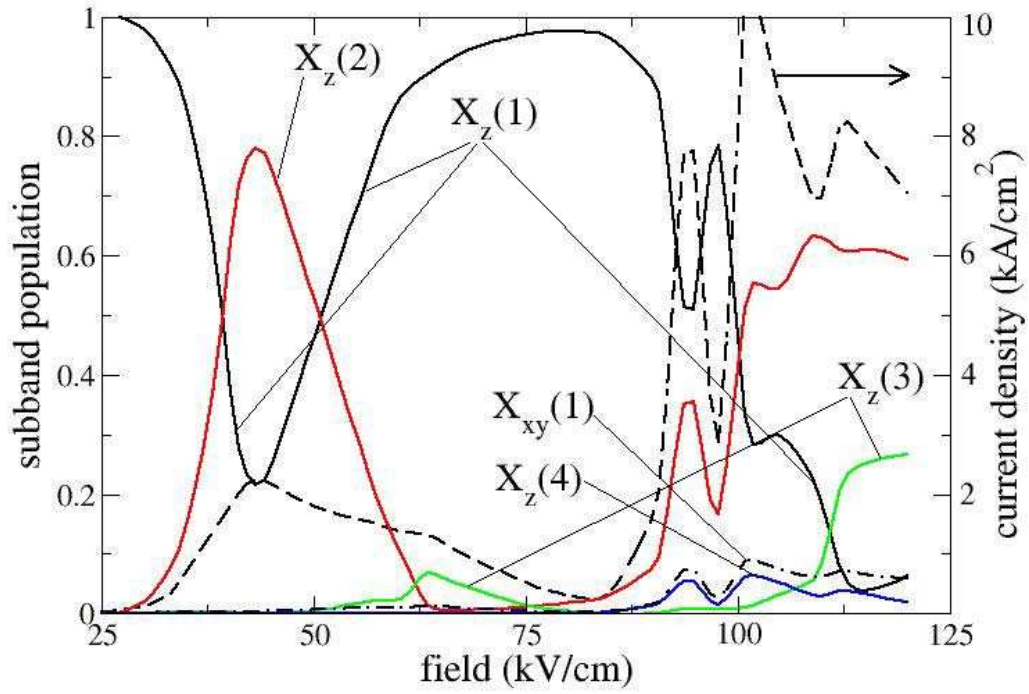


Fig.1.

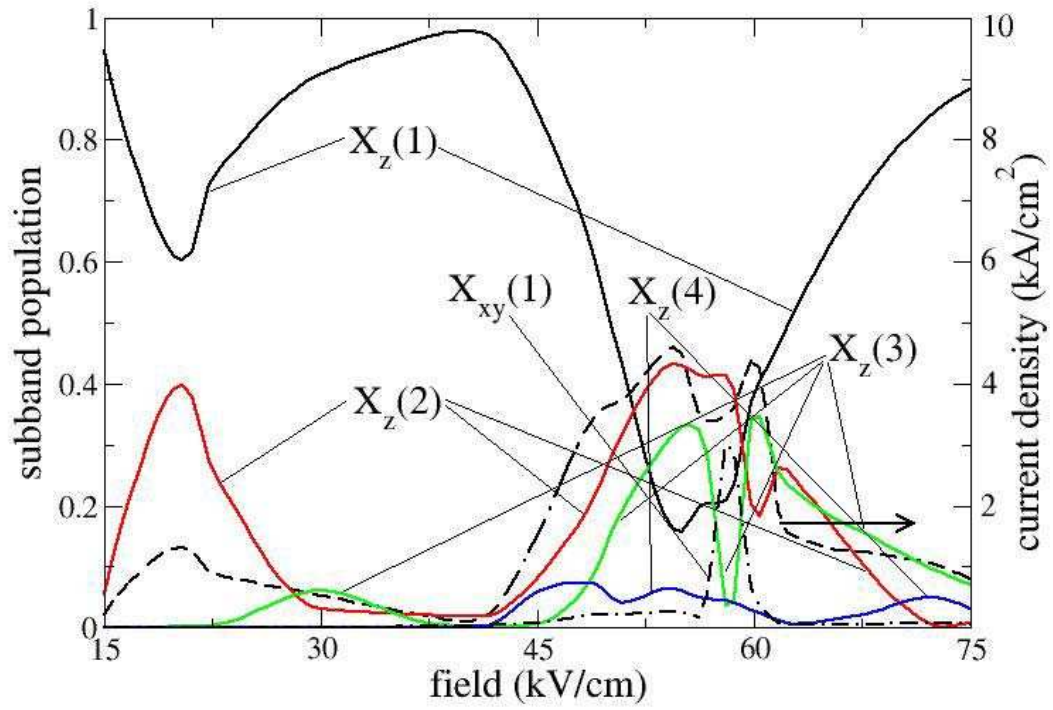


Fig.2.

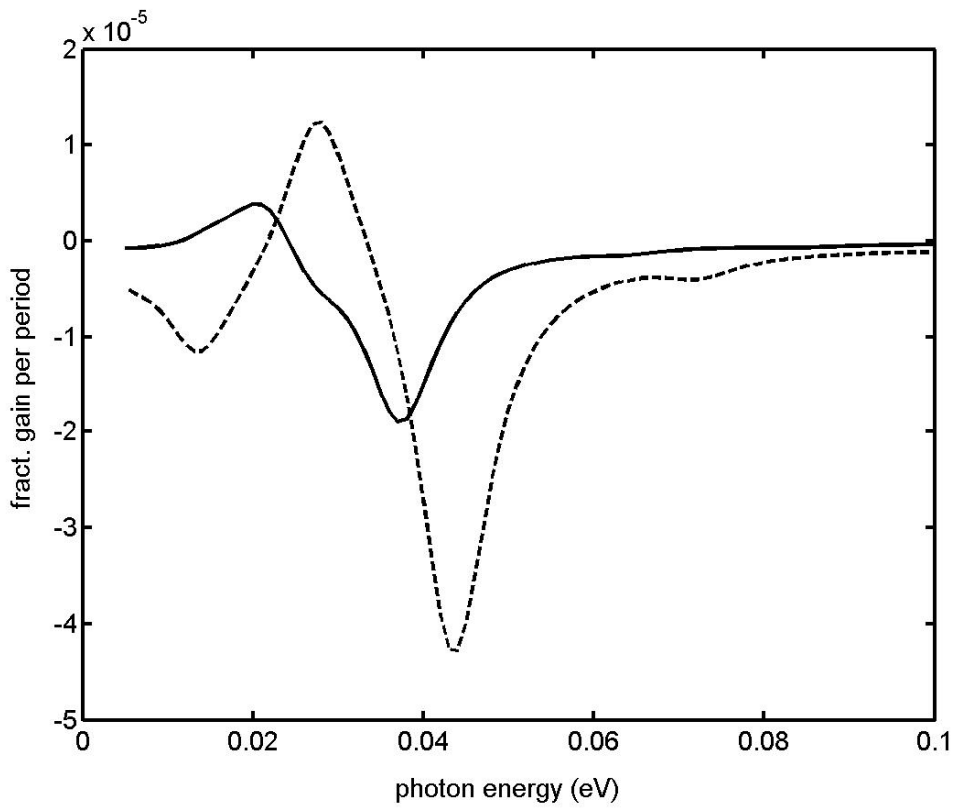


Fig.3.